



Simulation education utilizing phantom and angle reference guide in pulmonary nodule CT localization

Chiao-Yun Tsai^{a,b}, Stella Chin-Shaw Tsai^{c,d}, Guang-Qian Shen^e, Guan-Liang Robert Guo^e, Zhe-Luen Gerald Tsui^e, Ming-Yu Hsieh^{f,g}, Cadmus Yuan^e, Frank Cheau-Feng Lin^{a,b,g,*}

^a Department of Thoracic Surgery, Chung Shan Medical University Hospital, Taichung, Taiwan

^b Institute of Medicine, Chung Shan Medical University, Taichung, Taiwan

^c Superintendents' Office, Tungs' Taichung MetroHarbor Hospital, Taichung, Taiwan

^d Department of Postbaccalaureate Medicine, School of Medicine, National Chung Hsing University, Taichung, Taiwan

^e Department of Mechanical and Computer-Aided Engineering, Feng Chia University, Taichung, Taiwan

^f Department of Pediatric Surgery, Chung Shan Medical University Hospital, Taichung, Taiwan

^g School of Medicine, Chung Shan Medical University, Taichung, Taiwan

ARTICLE INFO

Keywords:

Pulmonary nodule
Computed tomography-guided localization
Phantom
Simulation
Medical education
Angle reference device

ABSTRACT

Objective: The incidence of sub-centimeter pulmonary nodules has been increasing along with the use of low-dose computed tomography (LDCT) as a screening tool for early lung cancer detection. In our institution, pulmonary nodule computed tomography-guided localization (PNCL) is performed preoperatively with the laser angle guided assembly (LAGA), an angle reference device. This study aims to investigate the efficacy of postgraduate education in a phantom simulation of PNCL, with or without LAGA.

Setting design: This prospective study was conducted in an academic hospital in Taiwan. Seven thoracic surgery residents and three experienced senior physicians were recruited to perform PNCL using a phantom simulation, with or without LAGA, for five nodules each and complete a questionnaire. Performance data were collected. χ^2 tests, Mann-Whitney *U* test, univariate and multivariate linear regression were used for statistical analyses.

Results: The confidence level increased from median 7 [range 1, 9] to 8, range [6,9] ($p = 0.001$) before and after the simulation education course. The scores of enhanced PNCL ability and course satisfaction were as high as 8 [5,9], and 9 [7,9]. LAGA enabled broader puncture angles (with 27.5° [0°,80°]; without 14° [0°, 80°], $p = 0.003$), a lower puncture frequency (with 1 [1,4]; without 2 [1,5], $p < 0.001$), and a smaller angle deviation (with 3° [0°,8°]; without 5° [0°,19°], $p = 0.002$). Pleural depth in millimeters was associated with increased puncture frequency (0.019 [0,010,0.028]) and procedure time (0.071' [0.018,0.123]'). The PNCL-experienced physicians performed the procedure in less time (-2.854' [-4.646',1.061]'). The traverse direction toward the mediastinum diminished the frequency (toward 1 [1,3]; away 1 [1,5], $p = 0.003$) and time (toward 7.5' [2',18]'; away 9' [3',31]', $p = 0.027$). The learning curve did not improve procedure performance after ten PNCL simulation rounds.

* Corresponding author. Department of Thoracic Surgery, Chung Shan Medical University Hospital, 110 Sec1 Jian-Guo N. Road, Taichung, 40201, Taiwan.

E-mail addresses: frnklin@gmail.com, frankcflin3@gmail.com (F.C.-F. Lin).

<https://doi.org/10.1016/j.heliyon.2023.e18329>

Received 16 November 2022; Received in revised form 11 July 2023; Accepted 13 July 2023

Available online 15 July 2023

2405-8440/© 2023 The Authors. Published by Elsevier Ltd. This is an open access article under the CC BY-NC-ND license (<http://creativecommons.org/licenses/by-nc-nd/4.0/>).

Conclusions: The phantom PNCL simulation education course increased the confidence level, enhanced residents' skill acquisition, and promoted learning satisfaction. The angle reference device helped improve the outcomes of the puncture frequency and reduced angle deviation.

1. Introduction

Performing medical interventional procedures or surgeries carries a certain level of risk, and those who are new to the field require some experience to attain a consistent learning curve and minimize the occurrence of complications to an acceptable level. Although the master-apprentice model is one of the most popular educational models [1], simulations have been developed to reduce the risks to patients during this learning process, which may include the use of an anthropomorphic phantom, virtual and actual reality, animal laboratory, computer-based simulation, and computer-assisted mannequins [2]. Various types of phantoms developed by trainers are commercially available and have been proven to be effective in medical education [1,3,4].

According to the 2018 Global Lung Cancer Incidence Map released by the World Health Organization, lung cancer has the highest global incidence and is the most frequently occurring type of cancer worldwide [5,6]. In the global ranking of lung cancer incidence, Taiwan held the 15th position and was the second highest in Asia, with North Korea being the only Asian country with a higher incidence rate. Early detection is essential for increasing the chances of survival in lung cancer, as with many other cancers. When diagnosed in the early stages, lung cancer can be highly curable, with cure rates as high as 80%–90% for patients with small tumors and early-stage cancer [7,8]. Still, as cancer develops and metastasizes regionally to the lymph nodes or distantly other parts of the body, the cure rate drops dramatically. Presently, low-dose computed tomography (LDCT) imaging is widely recognized as the most efficient imaging technique for early detection of lung cancer, and has become the primary diagnostic method for early lung cancer worldwide in clinical settings [8]. As a result, the incidence of pulmonary ground-glass nodules has also escalated. There is evidence in the literature to suggest that the use of LDCT can result in a reduction in mortality rates related to lung cancer [9]. According to health insurance data from Taiwan, there has been a noticeable rise in the incidence of early-stage lung cancer (stage 0 and 1) from 15.2% to 29.5% between 2007 and 2015 [10–12]. The trend is expected to continue, with a projected incidence rate of 32.95% by 2020. Following the favorable outcomes of TALENT study [13], Taiwan initiated a national lung cancer screening program, leading to an increased need for surgeries to remove subcentimeter nodules.

Therefore, correct identification, accurate diagnosis, and treatment of benign and malignant pulmonary nodules remain global issues. Moreover, these nodules are often very small, which can lead to difficulties in performing surgical interventions. Numerous localization methods have been developed for detecting lung tumors based on the available tools [14–17]. These methods include pulmonary nodule computed tomography-guided localization (PNCL), the use of a navigation system, and the hybrid operating room. To improve the visibility of nodules or mark their location in the lungs, tools such as blue dye, fluorescein dye, microcoil, and hookwire were utilized. Due to the high malignancy rate of approximately 85–90% associated with small pulmonary nodules, prompt diagnostic surgery is crucial for effective treatment [15,18–20]. With the help of PNCL, minimally invasive surgeries using needle scope and single port video-assisted thoracoscopic surgery (VATS) become feasible [21,22]. Nonetheless, PNCL is a risky procedure with 5–60% morbidity rate [23,24]. The failure of localization can result in the repeated wedge resection of the lung with massive lung volume loss, prolonged operation time, conversion to open surgery, missed tumor(s), metastasis, and/or the need for more surgeries [25,26].

The puncture angle was conventionally determined based on the physician's experience and tactile perception. Since 2018, our hospital has been employing computer tomography-guided localization and laser angle guidance assembly® technology (LAGA) to determine the puncture positioning of sub-centimeter pulmonary nodules before surgery. We reported the puncture hit rate of as high as 98.1% and the malignant pathological diagnosis rate of 87.7% [23]. However, performing this invasive procedure requires clinicians to receive education and training. To aid in clinical skills training and create a safer environment for clinical care, we developed custom-made phantoms for thoracic procedures. These phantoms have incorporated the mimicking of respiratory movements and can be particularly beneficial for novice clinicians [27]. This study aims to assess the educational effectiveness and benefits of a simulation course utilizing the innovative combination of the designed phantom and the angle reference guide in PNCL.

2. Methods

This is a single-center, nonrandomized controlled experimental trial with a within-subjects design followed by a questionnaire. For comparison, we recruited two attending physicians (a pulmonologist and a thoracic surgeon) and a surgical resident who practiced PNCL routinely, and another 7 of 14 surgical residents in our surgical department who were novice PNCL users. Each subject attempted 5 nodules with/without LAGA yielding a total of 50 nodules in each arm. With an alpha-error of 0.05 and power of 80%, the effective nodule numbers were 14 for each arm, calculated with G-power (3.1.8.2, Franz Faul, Uni Kiel, Germany). Each subject also completed a questionnaire before and after the course. This study was approved by the Institutional Review Board of Chung Shan Medical University Hospital (#CS13221). All subjects provided informed consent for their participation in the study and informed consent was obtained from the patients for the publication of their images.

2.1. Phantom (Fig. 1)

The preparation of the phantom of the pulmonary nodules in the thoracic cavity included: ten round flour dough lesions containing

iodine contrast agent as lung nodules (placed five lesions in the left and right lungs). Our real-world median size of the nodule was 6 mm, and we allowed 5 mm distance deviation. In this trial, the success targeting is defined of touch the nodule without any deviation allowed. The nodule was set to 10 mm in diameter and was actually 7–14 mm. They were distributed into the bilateral lungs, which were made of a jelly vacuum and placed in saline bags [28]. Additionally, the phantom also consisted of the chest wall made of polyvinyl chloride iron powder coating, the posterior spine represented by a polyethylene terephthalate plastic bottle, the intercostal muscles made of silicon, and the thoracic body skin made out of a polyurethane membrane.

2.2. CT scan

Philips CT Brilliance 64 (Hi Tech International Group, Inc., Florida) with the lung biopsy protocol was used in this study.

2.3. Laser angle guide assembly

The LAGA is a device that provides an angle reference according to the needle insertion planned on the CT image (Supplementary Fig. 1). The LAGA has been explained in more detail previously [29]. It indicates an angle that refers to the gravity with its frontal index line (Supplementary Fig. 1B), which is extended by its head laser, and was designed to point a red laser beam to the skin surface needle puncture point (SSNPP). Then the green portable laser is projected from the feet to the frontal index line, making the planned angle line at the SSNPP (Supplementary Fig. 1C).

2.4. Protocol of localization of the pulmonary nodules in the phantom

In the phantom PNCL simulation course, steps were followed according to the designed protocol, with and without LAGA (Supplementary Table 1) [29].

2.5. Questionnaires

The questionnaires were designed according to the Likert scale. The clinicians were asked about their confidence in performing the procedure and satisfaction with the course.

2.6. Data collection

The data of the volunteers were collected, including age, sex, and experience of localization.

The localization data about the size, location of the nodules, direction, angle planned, angle puncture, depth, time spent, and puncture frequency were also recorded. The requirements for the successful puncture hit of each lesion were met by the need to traverse the lesion but were not limited by the depth of the lesion. The frequency of puncture and the deviation of the actual puncture angle of the same lesion were recorded (Supplementary Fig. 2).

Table 1
Characteristics and outcomes with and without LAGA.

| | | Total | LAGA (+) | LAGA(–) | p |
|-------------------|------------------------|-----------|-----------|------------|---------|
| Demography | | | | | |
| Nodules | <i>N</i> | 100 | 50 | 50 | |
| Location | <i>Right</i> | 50 | 23 | 27 | 0.424 |
| | <i>Left</i> | 50 | 27 | 23 | |
| Size, mm | <i>Low/median/high</i> | 8-10-14 | 8-10-14 | 8-10-14 | 0.598 |
| | <i>0°</i> | 7 | 2 | 5 | |
| Direction | <i>inward</i> | 70 | 39 | 31 | 0.193 |
| | <i>outward</i> | 23 | 9 | 14 | |
| Angle planned,° | <i>Low/median/high</i> | 0/20/80 | 0/27.5/80 | 0/14/80 | 0.003* |
| Depth-skin, mm | <i>Low/median/high</i> | 36/60/104 | 36/55/104 | 39/63/100 | 0.005* |
| Depth-pleura, mm | <i>Low/median/high</i> | 21/42/88 | 23/38/85 | 21/46.5/88 | 0.019* |
| Outcomes | | | | | |
| Angle deviation,° | <i>Low/median/high</i> | 0/3/19 | 0/3/8 | 0/5/19 | 0.002* |
| Procedure Time | <i>Low/median/high</i> | 2/8/31 | 2/8/24 | 3/8/31 | 0.256 |
| Frequency | <i>Low/median/high</i> | 1/1/5 | 1/1/4 | 1/2/5 | <0.001* |
| | <i>1</i> | 67 | 43 | 24 | 0.001*† |
| | <i>2</i> | 22 | 5 | 17 | |
| | <i>3</i> | 8 | 1 | 7 | |
| | <i>4</i> | 2 | 1 | 1 | |
| | <i>5</i> | 1 | 0 | 1 | |

LAGA, Laser Angle Guide Assembly

Chi-square test and Mann-Whitney U Test, * p<0.05, †linear-by-linear association

2.7. Statistical analyses

After completing the data collection, typing, and decoding, the data were examined by a blinded statistics expert (Dr. JY Huang) using a statistical and mutual influence correlation analysis in SPSS for Windows version 18.0. The numerical data was tested with the Kolmogorov-Smirnov test for normality (Shapiro-Wilk test for age), with a non-normal distribution predominant (p values of angle 0.003, depth of skin 0.005, pleural 0.00, and age, time, and size <0.001 , respectively). The localizations with and without LAGA were compared using Chi-square tests for categorical data and Mann-Whitney U tests for continuous data. The puncture outcomes were all continuous data and analyzed with the Mann-Whitney U test, linear regression for univariate data and backward linear regression for multivariate data. The answers to the questionnaire on clinicians' confidence in performing localization before and after the course were compared using a paired-samples t -test. Finally, the potential reproducibility of the training program for LAGA was reviewed using a repeated measure analysis with a general linear model. A p -value of <0.05 was considered statistically significant.

3. Results

3.1. Characteristics of the volunteers, nodules, and localizations

Ten medical personnel participated in this study, including seven males and three females (Supplementary Table 2). Four, four, one, and one people were aged between 20 and 30, 30 and 40, 50 and 60, and 60 and 70 years old, respectively. The median age was 35 years old, with the youngest clinician being 28 and the oldest 67 years old. Among the ten personnel, three (a pulmonologist, a thoracic surgeon, a surgical resident) were experienced in PNCL, and seven were not experienced.

There were a total of 100 flour-lung lesions, with 50 each on the right and left sides of the lung (Table 1). The direction selection of the puncture angle in the zero-degree, inward, and outward directions accounted for 7%, 70%, and 23%, respectively. Flour-lung lesions ranged in size from 7.8 to 14 mm, with a median of 10 mm. The puncture angle measured by CT equipment was designed to be between 0° and 80° , with a median of 20° . The depth from the skin to the lesion ranged from 36 to 104 mm, with a median of 60 mm. The depth from the pleura to the lesion ranged from 21 to 88 mm, with a median of 42 mm. The puncture time required to complete each lesion ranged from 2 to 31 min, with a median of 8 min. The number of punctures required for puncture frequency with

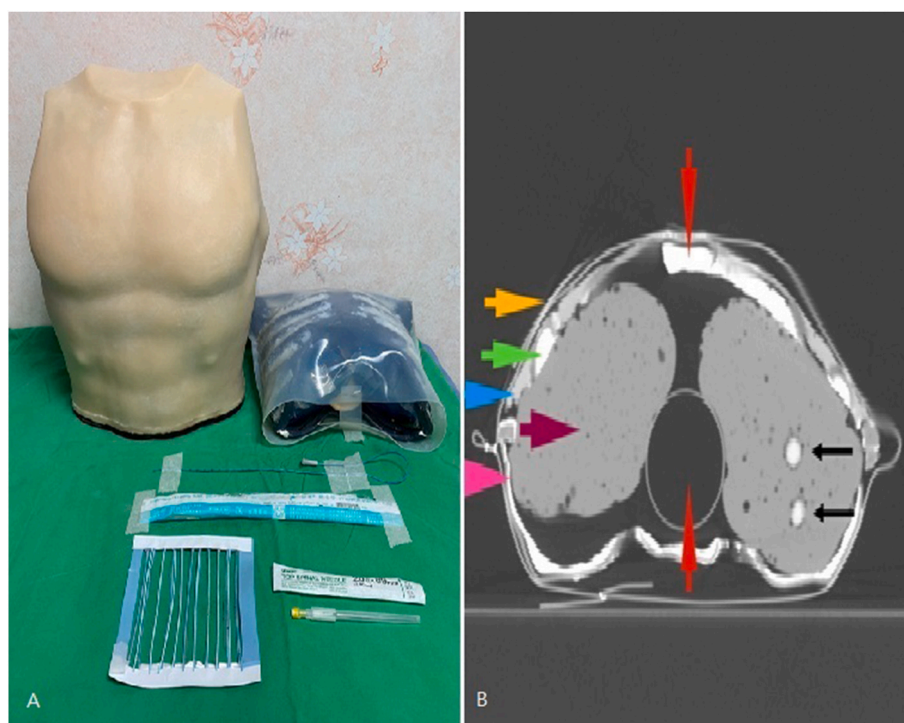


Fig. 1. The phantom and accessories A. Localization kit: radiopaque frame, 20-gauge needle, 89-mm spinal needle, and suction tube acting as a sheath to guide puncture depth. The phantom was made of a frame of thoracic skeleton. The lung, intercostal muscles, and skin were also prepared with pre-set pulmonary nodules. The ribs and pulmonary nodules were radiopaque. Lungs contained ten rounded and solid iodine-contrast flour doughs (8–14 mm) representing lung nodules. B. Phantom under the computed tomography (CT) scan. Anterior, sternum (red arrow pointing down); Posterior, spine (red arrow pointing up); Skin (yellow arrow); Rib cage (green arrow); Intercostal muscle (blue arrow); Lung (purple arrow); Pleural (pink arrow). (A) Two solid iodine-contrast flour dough lung nodules over the left side of the jelly-made lung (black arrow). (For interpretation of the references to colour in this figure legend, the reader is referred to the Web version of this article.)

and without the aid of LAGA ranged from one to five, with a median of one time (the frequency of the first puncture was 67%, second was 22%, third was 8%, fourth was 2%, and fifth was 1%). The angle of the puncture deviated from that planned by 0°–19° with a median of 3°.

3.2. Performance of pulmonary nodule CT-guided localization with and without LAGA

PNCL with or without LAGA showed that LAGA resulted in a higher first hit rate (accuracy) of 86% vs. 48%, $P < 0.001$, and a lower puncture frequency with medians (ranges) of 1 (1,4), and 2 (1,5), $p < 0.001$, with and without LAGA, respectively (Table 1). PNCL with LAGA also provided much better confidence to have a larger puncture angle planned with a median of 27.5° vs. 14°, $P = 0.003$, and the resulting angle deviations were much smaller (3° [maximum 8] vs. 5° [maximum 19], $p = 0.002$). The puncture depth was nearly 10 mm deeper in the LAGA (–) group with statistical significance (see Fig. 1).

3.3. Analyses of the factors affecting the puncture outcomes

Puncture frequency, puncture angle deviation from the planned angle, and procedure time were the three outcomes that appeared to affect the puncture outcomes (Fig. 2A–C). This technology was not found to be limited by the age and sex of the volunteers and the location and size of the nodules (Table 2). However, there was a significant difference between those that were experienced versus inexperienced in terms of the puncture time with a median (range) of 6.5 (2–15) vs. 8.0 (3–31) min, $P = 0.009$, respectively.

The design of the direction of the puncture angle significantly affected the puncture frequency and puncture time. It took a median of 7 min to hit the lesion in the zero-degree direction, 7.5 min in the inward direction, and 9 min in the outward direction ($P = 0.027$).

The puncture frequency was affected by the depth of the skin and pleura to the lesion (both $p < 0.001$). The puncture time was also affected by the depth of the skin and pleura to the lesion ($p = 0.007$ and 0.002 , respectively). The depth of the pleura had more influence on the outcomes than that of the skin, according to the odds ratio and p-value.

The factors that could affect the three performance outcomes were tested with multivariate linear regression. The puncture frequency was increased by the depth of the pleura and diminished by the use of LAGA with a B[β , Regression coefficients] (95% CI [confidence interval]) of 0.019 (0.010, 0.028) and -0.439 (-0.726 , -0.151), respectively. LAGA, as an angle reference, reduced the angle deviation with a B of -2.740 . The multivariate analyses of the puncture time required for each lesion's hit rate were similar to the univariate analysis. The outward direction of the puncture design had a B of 2.321 and 95% CI of 0.741, 3.901. Without the aid of LAGA, each lesion hit took a medium of 7 min to complete. In contrast, with the assistance of LAGA, each lesion hit took a median of 8 min to complete. However, no statistical significance was found in the multivariate analyses ($P = 0.256$). This study also showed that experienced individuals required less puncture time to achieve the hit completion time for each lesion, and the pleural depth was an associated factor with a B of 0.071 with $p = 0.009$.

3.4. Questionnaire and learning curves of the pulmonary nodule CT-guided localization simulation course

The analysis of the questionnaire answers before and after the training course showed that the confidence of successful PNCL was increased from a median (minimum, maximum) of 7 (1,9) to 8 (5,9), $p = 0.001$. It can be observed that the low confidence was a minimum of 6 from 1 of 9 scores (Table 3). Most volunteers gave a high score for the course promoting PNCL ability (median of 8/9). Only three of the ten volunteers evaluated it as of moderate value. No volunteers scored the course as being of no help. The satisfaction

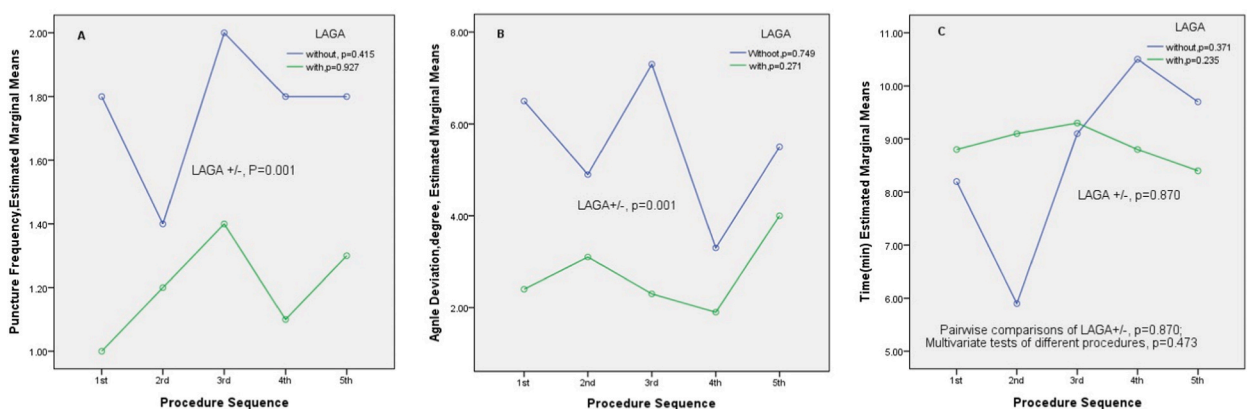


Fig. 2. Analyses of the learning curves of puncture outcomes A. Puncture frequency. Tests of between-group with and without LAGA effects, $p = 0.001$. Tests of within-group contrast, linear, with LAGA $p = 0.902$ intraclass correlation coefficient (ICC) -1.174 , without LAGA $p = 0.414$ ICC 0.133 . B. Angle deviation. Tests of between-group with and without LAGA effects, $p = 0.001$. Tests of within-group contrast, linear, with LAGA $p = 0.271$ ICC -0.263 , without LAGA $p = 0.749$ ICC 0.083 . C. Procedure time as outcome. Tests of between with and without LAGA effects, $p = 0.0087$. Tests of within group contrast, linear, With LAGA $p = 0.235$ ICC 0.693 , Without LAGA $p = 0.371$ ICC 0.406 .

Table 2
Factors affecting localization outcomes.

| | | B (95% CI) | Frequency | P | Angle Deviation (degree) | P | Procedure Time (minutes) | P |
|------------------------------|---------|-----------------|-------------------------|----------|--------------------------|----------|--------------------------|--------|
| | | | | | | | | |
| Age | | | −0.001 (−0.014, 0.013) | 0.919 | −0.002 (−0.094, 0.090) | 0.66 | −0.006 (−0.081, 0.070) | 0.885 |
| Experience | With | Low/median/high | 1/1/3 | 0.732 | 0/3.5/19 | 0.98 | 2/6.5/15 | 0.009* |
| | Without | Low/median/high | 1/1/5 | | 0/3/16 | | 3/8/31 | |
| Gender | Male | Low/median/high | 1/1/5 | 0.931 | 0/3/12 | 0.18 | 3/8/31 | 0.129 |
| | Female | Low/median/high | 1/1/4 | | 0/4/19 | | 2/7/18 | |
| Location | Right | Low/median/high | 1/1/3 | 0.642 | 0/4/16 | 0.27 | 3/8/18 | 0.852 |
| | Left | Low/median/high | 1/1/3 | | 0/3/19 | | 2/8/31 | |
| | 0° | Low/median/high | 1/1/3 | | 1/1/9 | | 4/7/13 | |
| Direction | Inward | Low/median/high | 1/1/3 | 0.003* | 0/3/19 | 0.100 | 2/7.5/18 | 0.027* |
| | Outward | Low/median/high | 1/1/5 | | 0/5/16 | | 3/9/31 | |
| LAGA | With | Low/median/high | 1/1/3 | 0.001* | 0/3/8 | 0.002* | 2/8/24 | 0.256 |
| | Without | Low/median/high | 1/2/5 | | 0/5/19 | | 2/7/31 | |
| Nodule Size | | B (95% CI) | −0.019 (−0.138, 0.091) | 0.752 | 0.064 (−0.738, 0.867) | 0.87 | −0.68 (−0.72, 0.58) | 0.838 |
| Depth skin | | B (95% CI) | 0.020 (0.011, 0.029) | < 0.001* | −0.010 (−0.076, 0.057) | 0.78 | 0.073 (0.020, 0.126) | 0.007* |
| Depth pleura | | B (95% CI) | 0.022 (0.012, 0.031) | < 0.001* | −0.018 (−0.089, 0.092) | 0.61 | 0.087 (0.031, 0.142) | 0.002* |
| Angle planned | | B (95% CI) | −0.002 (−0.011, 0.006) | 0.562 | −0.061 (−0.117, −0.004) | 0.035* | −0.020 (−0.067, 0.027) | 0.403 |
| Multivariate Analyses | | | | | | | | |
| LAGA | | B (95% CI) | −0.439 (−0.726, −0.151) | 0.003* | −2.740(−4.115, −1.365) | < 0.001* | | |
| Depth pleura | | B (95% CI) | 0.019 (0.010, 0.028) | < 0.001* | | | 0.071 (0.018, 0.123) | 0.009* |
| Experienced | | B (95% CI) | | | | | −2.854 (−4.646, −1.061) | 0.002* |
| Direction | | B (95% CI) | | | | | 2.321 (0.741, 3.901) | 0.004* |

LAGA, Laser Angle Guide Assembly. Edited.

score was the highest, with 9/9 as the median and seven as the lowest score.

Furthermore, repeated measures analysis of the learning curve revealed that decreased puncture frequency depended on the use of LAGA rather than repeated PNCL practice (Fig. 2). The learning curve did not appear to decrease according to the puncture order, but the learning curve differed between LAGA-assisted and non-assisted procedures with a p-value of 0.001. The learning curve of angle deviation showed similar results. The learning curve without LAGA seemed to decrease by the fourth and fifth punctures compared to the second and third punctures (p = 0.749). However, the fifth trial with the LAGA group was higher than the previous four times (p = 0.271), and the learning curve with and without LAGA separated with a p-value of 0.001.

Table 3
Questionnaire for phantom pulmonary nodule CT-guided localization simulation course.

| Likert score | 1 | 2 | 3 | 4 | 5 | 6 | 7 | 8 | 9 | Range | Median | p |
|---|---|---|---|---|---|---|---|---|---|-------|--------|--------------------|
| Confidence of success PNCL, before course | 1 | | 3 | | | | 3 | 2 | 1 | 1, 9 | 7 | 0.001 ^a |
| Confidence of success PNCL, after course | | | | | | 2 | 2 | 2 | 4 | 6, 9 | 8 | |
| Promotion of PNCL ability | | | | | 1 | 2 | 1 | 2 | 4 | 5, 9 | 8 | |
| Course satisfaction | | | | | | | 1 | 3 | 6 | 7, 9 | 9 | |

PNCL pulmonary nodule CT-guided localization. Likert score 1–3 Low, 7–9 high.

^a paired t t-test.

4. Discussion

The educational course on PNCL simulation effectively enhanced the competence and self-assurance of both seasoned physicians and trainee residents in performing PNCL. Statistical analysis showed that the participant's confidence before and after the procedure and after training had significantly improved ($P = 0.004$). Therefore, this course can be expected to help reduce the learning curve.

Animal models are often employed for surgical training, but the usage of such models is constrained by the unavailability of animal-specific CT for PNCL and anesthesia facilities. The high cost associated with PNCL animal laboratory models is mostly related to the development of new techniques [30,31]. While digital courses have been organized for educating individuals in bronchoscopy and chest tube insertion procedures, no such courses have been developed for PNCL training [32]. Virtual reality has been used in surgical skill training with robotic simulators [33]. Anthropomorphic phantom is one of the good choices for simulation in addition to virtual reality, actual reality, and animal laboratory models. It was used to simulate radiation dosage, respiratory-gated technique, lung ablations, and PNCL [2–4,27,34–36]. In fact, a phantom PNCL course combined with augmented reality showed promising results, with 12 out of 16 clinicians reporting increased confidence in performing PNCL [29]. Similarly, a phantom model created through 3D printing for CT-guide localization was tested with ten doctors, resulting in great satisfaction [35]. While educational courses using animal models may not always mimic reality, the use of actual reality, virtual reality, and anthropomorphic phantom models can potentially offer a more suitable alternative for PNCL training. These findings validate the merit of incorporating the current phantom model in PNCL educational courses. Performing procedures on a phantom is typically considered easier than on a real patient due to the absence of potential complications such as bleeding or pneumothorax. In addition, the only structure that needs to be avoided is the rib, and there are no respiratory or circulatory movements in the phantom that could cause deviations in the targeting of nodules. Unlike real patients, phantoms do not experience pain, fatigue, or fear, which can cause body movements and make the procedure more challenging. Engaging in practice on a phantom prior to working with real patients is a beneficial step towards achieving success in the actual procedure on a real person.

Another research goal of this study is to investigate how various factors impact the puncture process, as well as to assess the benefits and drawbacks associated with targeting sub-centimeter pulmonary nodules with or without LAGA. LAGA influences the PNCL from the initial planning stage. The planned angle differences between the actual puncture angle with or without LAGA in the 100 flour-lung lesions were analyzed. We prefer the puncture angle to be right-on-gravity (0°). Without LAGA, the median planned puncture angle was 14° , and the median planned puncture angle with LAGA was 27.5° ($P = 0.003$, Table 1). Moreover, it is possible to use larger puncture angles, even assuming better puncture confidence and potential when crossing the danger zone. Results from the current study demonstrated that the use of LAGA also improved puncture frequency and angle deviation outcomes. In the real world, various medical protocols and clinical practices are influenced by the medical insurance and national medical health economy systems around the world. Advanced procedural spaces such as hybrid operating rooms, which combine traditional operating rooms with image-guided interventional suites, are recent advancements that require a multidisciplinary team of clinicians to meet the complex needs of patients. LAGA has been found to provide a very precise angle reference with a much lower cost than the Pheno or Zeego of the hybrid OR. Compared to the intra-bronchial navigation system, the LAGA PNCL system is more accurate. However, it was not commercially available and was only available with the authorization of our institution. To circumvent this issue, in the PNCL workshops we hosted, a protractor app on a mobile phone with an extension indicator has also proved beneficial (Supplementary Fig. 1E).

There have been reports that the frequency of multiple punctures has increased the rate of complications caused by puncture injury by up to 40%, such as pneumothorax [23,24,37]. The distance deviation from the target to the tip of the puncture needle is 'depth of puncture' $\times 2\sin(\theta)$, θ = angle deviation. The mathematical formula indicates that angle deviation and pleural depth are the key factors that determine the puncture frequency. Specifically, when there is a greater deviation in distance, more repeated punctures are required. The angle deviation and pleura depth both affect the puncture frequency, as seen in the current study with a B of 0.116 and 0.119 and a p-value of <0.001 (Table 1). The puncture depth of the pleura and skin were mentioned in most research as prognostic factors [38–43]. However, this depth is determined by the nodule location, ribs, and structures throughout the puncture route rather than the operator. The precision of the angle is a controllable factor with the assistance of an angle reference device. Nevertheless, this factor is seldom discussed in the literature [41] probably because there was no effective tool to control it, and it was rarely recorded in studies. As the angle deviation is an outcome variable and not included in the regression of factors associated with puncture frequency, the LAGA and pleural depth were the factors that affected puncture frequency with an OR (95% CI) of -0.439 ($-0.726, -0.151$) and 0.019 ($0.010, 0.028$), respectively (Table 2). The first hit rate with and without LAGA was 86% vs. 48%, with almost twice the success rate. Furthermore, the median hit frequency was 1 and 2 with and without LAGA, respectively. This is the first study to show that an angle reference device can reduce the puncture frequency of PNCL in the training course. In addition, the angle reference device was also the only factor associated with the angle deviation as expected (Table 2). The first-puncture hit rate with and without LAGA was 86% vs. 48%, with almost twice the success rate. Furthermore, the median hit frequency was 1 and 2 with and without LAGA, respectively. This study is the first to demonstrate that the use of an angle reference device during training courses can decrease the frequency of punctures required for PNCL. In addition, the angle reference device was also the only factor associated with the angle deviation as expected (Table 2). The use of LAGA affected the frequency and angle deviation more than the experience of performing ten PNCLs (Table 2). Taken together, these results suggested that using LAGA could reduce the amount of learning and experience required to achieve good outcomes. According to the literature published by Yin-Kai Chao et al., the time required for the localization procedure was affected by the skin-to-lesion depth ($P = 0.007$) and pleural-to-lesion depth ($P = 0.002$) [17]. CT fluoroscopy rather than CT for PNCL also reduced procedure times [44]. The puncture time required to complete a lesion hit rate does not appear to be affected by the location of the lesion, the size of the sub-centimeter lesion, the planned puncture angle, or the age and sex of the staff

(Table 2). In exploring 100 flour-lung lesions, the design of empirical values for puncture frequency and angle deviation was not limited by experience-dependent effects. However, a significantly better puncture time was found for experienced clinicians ($P = 0.009$). The findings suggest that this technology has the potential to benefit inexperienced staff. Although setting up LAGA may require additional time, the time required for the LAGA group was not significantly longer, which was likely compensated for by the increased precision and reduction in the number of required punctures.

Our study is subject to several limitations, including the short learning period and the potential risks associated with simulating procedures in a controlled environment. Furthermore, the study did not establish the reasons behind the correlation between the puncture localization hit rate and various influencing factors. To enhance the realism of the training, future iterations of the phantom could include additional organs, breathing patterns, blood vessels, trachea, mediastinal organs, and diaphragmatic movements. The training program could also be improved by incorporating a buffer mechanism to limit the range of the puncture angle depth. Additionally, it would be valuable to investigate whether setting a limit on the number of punctures allowed during training could improve the accuracy of puncture hit rate and enhance the degree of realistic execution in trainees. Our team plans to explore the future development of angle reference devices with artificial intelligence and automated features. As previously mentioned in the introduction, virtual reality has proven useful in education, and augmented reality techniques could also be applied to localization simulations. Therefore, we believe that these technologies could be excellent options for enhancing localization simulation and training.

The techniques described in this study offer a cost-effective, safe, and efficient alternative to traditional methods, with a reduced learning curve. Specifically, in a separate study, we have introduced a replacement method that utilized an online Protractor-APP system and a metal stick to form the angle-axis for PNCL procedures under CT guidance, which provided a clear localization for the puncture as expected (Supplementary Fig. 1E). We created a practical clinical program using the thoracic phantom, CT-guided with the LAGA device, Protractor-APP system, and puncture kits. In addition, we successfully conducted a CT localization hands-on workshop, and the feedback from the participants was excellent [36].

5. Conclusion

The anthropomorphic phantom PNCL educational simulation course was found to be effective in the postgraduate training of clinicians. The use of the angle reference device improved the accuracy, precision, puncture frequency, and safety of lung nodule localization for both experienced and inexperienced staff. Hence, we recommend the use of the angle reference device for residents-in-training and advocate for its application in routine clinical practice. Moreover, LAGA and mobile phone models could be applied in remote areas with limited access to medical services and equipment. We anticipate further enhancement on both the localization technique and the training system with artificial intelligence and automated features for improved outcomes and better overall patient care. Finally, future research is underway to explore the prospects of PNCL and LAGA technology in lung cancer treatment and other lung surgeries.

Funding

The research was funded by the Ministry of Education, Taiwan (Grant#PMN1110052) and Tungs' Taichung MetroHarbor Hospital (Grant#TTMHH-R1120009).

Author contribution statement

Chiao-Yun Tsai and Frank Chau-Feng Lin: Conceived and designed the experiments; Performed the experiments; Wrote the paper.
Stella Chin-Shaw Tsai: Contributed reagents, materials, analysis tools or data; Wrote the paper.
Guang-Qian Shen: Performed the experiments.
Guan-Liang Robert Guo, Zhe-Luen Gerald Tsui, Ming-Yu Hsieh and Cadmus Yuan: Contributed reagents, materials, analysis tools or data.

Data availability statement

Data will be made available on request.

Additional information

Supplementary content related to this article has been published online at [URL].

Declaration of competing interest

The authors declare no conflict of interest.

Acknowledgment

We would like to thank Tsai-Ling Hsieh for editorial and technical assistance.

We would like to thank Dr. Jin-Yang Huang for statistical consultations. The raw data was published at Lin, Frank (2023), "Phantom", Mendeley Data, V1, <https://doi.org/10.17632/hgdf4jwjsxm.1>.

Appendix A. Supplementary data

Supplementary data to this article can be found online at <https://doi.org/10.1016/j.heliyon.2023.e18329>.

References

- [1] Z.A. Miller, A. Amin, J. Tu, et al., Simulation-based training for interventional radiology and opportunities for improving the educational paradigm, *Tech. Vasc. Intervent. Radiol.* 22 (1) (2019) 35–40.
- [2] S. Mirza, S. Athreya, Review of simulation training in interventional radiology, *Acad. Radiol.* 25 (4) (2018) 529–539.
- [3] J. Wilson, L. Ng, V. Browne, et al., An easy-to-make, low-cost ultrasound phantom for simulation training in abscess identification and aspiration, *J. Ultrasound Med.* 36 (6) (2017) 1241–1244.
- [4] S. Mesko, B.V. Chapman, C. Tang, et al., Development, implementation, and outcomes of a simulation-based medical education (sbme) prostate brachytherapy workshop for radiation oncology residents, *Brachytherapy* 19 (6) (2020) 738–745.
- [5] E. Goodarz, M. Sohrabivafa, H.A. Adineh, et al., Geographical distribution global incidence and mortality of lung cancer and its relationship with the human development index(hdi); an ecology study in 2018, *World Cancer Research Journal* 6 (2019) e1354.
- [6] J.A. Barta, C.A. Powell, J.P. Wisnivesky, Global epidemiology of lung cancer, *Ann Glob Health* 85 (1) (2019).
- [7] P. Goldstraw, K. Chansky, J. Crowley, et al., The iaslc lung cancer staging project: proposals for revision of the tnm stage groupings in the forthcoming (eighth) edition of the tnm classification for lung cancer, *J. Thorac. Oncol.* 11 (1) (2016) 39–51.
- [8] S. Blandin Knight, P.A. Crosbie, H. Balata, et al., Progress and prospects of early detection in lung cancer, *Open Biol* 7 (9) (2017).
- [9] D.R. Aberle, A.M. Adams, C.D. Berg, et al., Reduced lung-cancer mortality with low-dose computed tomographic screening, *N. Engl. J. Med.* 365 (5) (2011) 395–409.
- [10] J.C. Hsu, C.F. Wei, S.C. Yang, et al., Lung cancer survival and mortality in taiwan following the initial launch of targeted therapies: an interrupted time series study, *BMJ Open* 10 (5) (2020), e033427.
- [11] R. Govindan, N. Page, D. Morgensztern, et al., Changing epidemiology of small-cell lung cancer in the United States over the last 30 years: analysis of the surveillance, epidemiologic, and end results database, *J. Clin. Oncol.* 24 (28) (2006) 4539–4544.
- [12] C.A. Reade, A.K. Ganti, Egfr targeted therapy in non-small cell lung cancer: potential role of cetuximab, *Biologics* 3 (2009) 215–224.
- [13] P. Yang, Ps01.02 national lung cancer screening program in taiwan: the talent study, *J. Thorac. Oncol.* 16 (3) (2021) S58.
- [14] E. De Kerviler, D. Gossot, J. Frijia, Localization techniques for the thoracoscopic resection of pulmonary nodules, *Int. Surg.* 81 (1996) 241.
- [15] O. Awais, M.R. Reidy, K. Mehta, et al., Electromagnetic navigation bronchoscopy-guided dye marking for thoracoscopic resection of pulmonary nodules, *Ann. Thorac. Surg.* 102 (1) (2016) 223–229.
- [16] Y.R. Chen, K.M. Yeow, J.Y. Lee, et al., Ct-guided hook wire localization of subpleural lung lesions for video-assisted thoracoscopic surgery (vats), *J. Formos. Med. Assoc.* 106 (11) (2007) 911–918.
- [17] Y.K. Chao, K.T. Pan, C.T. Wen, et al., A comparison of efficacy and safety of preoperative versus intraoperative computed tomography-guided thoracoscopic lung resection, *J. Thorac. Cardiovasc. Surg.* 156 (5) (2018) 1974–1983.e1.
- [18] Y.F. Fu, M. Zhang, W.B. Wu, et al., Coil localization-guided video-assisted thoracoscopic surgery for lung nodules, *J. Laparoendosc. Adv. Surg. Tech.* 28 (3) (2018) 292–297.
- [19] T. Iguchi, T. Hiraki, H. Gohara, et al., Ct fluoroscopy-guided preoperative short hook wire placement for small pulmonary lesions: evaluation of safety and identification of risk factors for pneumothorax, *Eur. Radiol.* 26 (1) (2016) 114–121.
- [20] Y. Yoshida, S. Inoh, T. Murakawa, et al., Preoperative localization of small peripheral pulmonary nodules by percutaneous marking under computed tomography guidance, *Interact. Cardiovasc. Thorac. Surg.* 13 (1) (2011) 25–28.
- [21] K.W. Doo, H.S. Yong, H.K. Kim, et al., Needlescopic resection of small and superficial pulmonary nodule after computed tomographic fluoroscopy-guided dual localization with radiotracer and hookwire, *Ann. Surg. Oncol.* 22 (1) (2015) 331–337.
- [22] D. Gonzalez-Rivas, E. Fieira, M. Delgado, et al., Uniportal video-assisted thoracoscopic lobectomy, *J. Thorac. Dis.* 5 (Suppl 3) (2013) S234–S245.
- [23] S.C. Tsai, T.C. Wu, Y.L. Lai, et al., Preoperative computed tomography-guided pulmonary nodule localization augmented by laser angle guide assembly, *J. Thorac. Dis.* 11 (11) (2019) 4682–4692.
- [24] C.Y. Lin, C.C. Chang, L.T. Huang, et al., Computed tomography-guided methylene blue localization: single vs. Multiple lung nodules, *Front. Med.* 8 (2021), 661956.
- [25] K. Suzuki, K. Nagai, J. Yoshida, et al., Video-assisted thoracoscopic surgery for small indeterminate pulmonary nodules: indications for preoperative marking, *Chest* 115 (2) (1999) 563–568.
- [26] S. McDermott, F.J. Fintelmann, A.J. Bierhals, et al., Image-guided preoperative localization of pulmonary nodules for video-assisted and robotically assisted surgery, *Radiographics* 39 (5) (2019) 1264–1279.
- [27] K. Bolwin, B. Czekalla, L.J. Frohwein, et al., Anthropomorphic thorax phantom for cardio-respiratory motion simulation in tomographic imaging, *Phys. Med. Biol.* 63 (3) (2018), 035009.
- [28] D. Amiras, T.J. Hurixkens, D. Figueroa, et al., Augmented reality simulator for ct-guided interventions, *Eur. Radiol.* 31 (12) (2021) 8897–8902.
- [29] F.C. Lin, S.C. Tsai, H.T. Tu, et al., Computed tomography-guided localization with laser angle guide for thoracic procedures, *J. Thorac. Dis.* 10 (6) (2018) 3824–3828.
- [30] D. Jangra, T. Powell, S.E. Kalloger, et al., Ct-directed microcoil localization of small peripheral lung nodules: a feasibility study in pigs, *J. Invest. Surg.* 18 (5) (2005) 265–272.
- [31] H. Wada, J. Zheng, A. Gregor, et al., Intraoperative near-infrared fluorescence-guided peripheral lung tumor localization in rabbit models, *Ann. Thorac. Surg.* 107 (1) (2019) 248–256.
- [32] C. Rieder, M. Schwenke, T. Pätz, et al., Evaluation of a numerical simulation for cryoablation - comparison with bench data, clinical kidney and lung cases, *Int. J. Hyperther.* 37 (1) (2020) 1268–1278.
- [33] R. Chen, P. Rodrigues Armijo, C. Krause, et al., A comprehensive review of robotic surgery curriculum and training for residents, fellows, and postgraduate surgical education, *Surg. Endosc.* 34 (1) (2020) 361–367.
- [34] M. Meier-Meitingner, M. Nagel, W. Kalender, et al., [computer-assisted navigation system for interventional ct-guided procedures: results of phantom and clinical studies], *Röfo* 180 (4) (2008) 310–317.

- [35] P. Jahnke, F.B. Schwarz, M. Ziegert, et al., A radiopaque 3d printed, anthropomorphic phantom for simulation of ct-guided procedures, *Eur. Radiol.* 28 (11) (2018) 4818–4823.
- [36] F.C.-F. Lin, G.-Z. Wang, C.-Y. Tsai, *Ct Localization Workshop/the 2nd Asia Ggn-Early Lung Adenocarcinoma Symposium*, Taiwan Association of Thoracic & Cardiovascular Surgery, 2021.
- [37] F. Yao, J. Wang, J. Yao, et al., Reevaluation of the efficacy of preoperative computed tomography-guided hook wire localization: a retrospective analysis, *Int. J. Surg.* 51 (2018) 24–30.
- [38] H.K. Bungay, J. Berger, Z.C. Traill, et al., Pneumothorax post ct-guided lung biopsy: a comparison between detection on chest radiographs and ct, *Br. J. Radiol.* 72 (864) (1999) 1160–1163.
- [39] C.M. Heyer, S. Reichelt, S.A. Peters, et al., Computed tomography-navigated transthoracic core biopsy of pulmonary lesions: which factors affect diagnostic yield and complication rates? *Acad. Radiol.* 15 (8) (2008) 1017–1026.
- [40] S.E. Loh, D.D. Wu, S.K. Venkatesh, et al., Ct-guided thoracic biopsy: evaluating diagnostic yield and complications, *Ann. Acad. Med. Singapore* 42 (6) (2013) 285–290.
- [41] H. Saji, H. Nakamura, T. Tsuchida, et al., The incidence and the risk of pneumothorax and chest tube placement after percutaneous ct-guided lung biopsy: the angle of the needle trajectory is a novel predictor, *Chest* 121 (5) (2002) 1521–1526.
- [42] L.I. Jae, I.H. June, Y. Miyeon, et al., Percutaneous core needle biopsy for small (≤ 10 mm) lung nodules: accurate diagnosis and complication rates, *Diagn Interv Radiol* 18 (6) (2012) 527–530.
- [43] N. Asai, Y. Kawamura, I. Yamazaki, et al., Is emphysema a risk factor for pneumothorax in ct-guided lung biopsy? *SpringerPlus* 2 (1) (2013) 196.
- [44] D. Gianfelice, L. Lepanto, P. Perreault, et al., Value of ct fluoroscopy for percutaneous biopsy procedures, *J. Vasc. Intervent. Radiol.* 11 (7) (2000) 879–884.